ORIGINAL ARTICLE

CrossMark

Red bone marrow dose estimation using several internal dosimetry models for prospective dosimetry-oriented radioiodine therapy

Mohammad Abuqbeitah[1] · Mustafa Demir[1] · İffet Çavdar[2] · Handan Tanyildizi[2,3] · Nami Yeyin[1] · Lebriz Uslu-Beşli[1] · Levent Kabasakal[1] · Nazenin İpek Işıkcı[4] · Kerim Sönmezoğlu[1]

Abstract

The aim of the present study was to review the available models developed for calculating red bone marrow dose in radioiodine therapy using clinical data. The study includes 18 patients (12 females and six males) with metastatic differentiated thyroid cancer. Radioiodine tracer of 73 ± 16 MBq ^{131}I was orally administered, followed by blood sampling (2 ml) and whole-body scans (WBSs) done at several time points (2, 6, 24, 48, 72, and ≥ 96 h). Red bone marrow dose was estimated using the OLINDA/EXM 1.0, IDAC-Dose 2.1, and EANM models, the models developed by Shen and co-workers, Keizer and co-workers and Siegel and co-workers, and Traino and co-workers, as well as the single measurement model (SMM). The results were then compared to the standard reference model Revised Sgouros Model (RSM) reported by Wessels and co-workers. The mean dose deviations of the Traino, Siegel, Shen, Keizer, OLINDA/EXM, EANM, SMM, and IDAC-Dose 2.1 models from the RSM were -17%, -24%, 6%, -29%, -15%, 40%, 48%, and -8%, respectively. The statistical analysis demonstrated no significant difference between the results obtained with the RSM and with those obtained with the Shen, Traino, OLINDA/EXM, and IDAC-Dose 2.1 models (t test; $p_{value} > 0.05$). However, a significant difference was found between RSM doses and those obtained with the EANM, SMM, and Keizer models (t test; $p_{value} < 0.05$). The correlation between red marrow dose from the SMM and EANM models was modest ($R^2 = 0.65$), while the crossfire dose calculated with the OLINDA/EXM and IDAC-Dose 2.1 models were in good agreement with each other and with the reference model. The findings obtained indicate that most of the dosimetry models can be used for a reliable dosimetry, and the calculated total body doses can be considered as a reliable non-invasive option for a conservative activity planning. In addition, the excellent performance of the IDAC-Dose 2.1 model will be of particular importance for a practical and accurate dosimetry, with the advantages of allowing for the use of realistic advanced phantoms and updated dose fractions, and of providing information about the blood dose contribution to the red bone marrow.

Keywords Red marrow · Dosimetry models · Radioiodine therapy · IDAC-Dose 2.1

✉ Mohammad Abuqbeitah
qbeta95@hotmail.com

1   Cerrahpasa Faculty of Medicine, Department of Nuclear Medicine, Istanbul University, Istanbul, Turkey

2   Science Faculty, Department of Nuclear Physics, Istanbul University, Istanbul, Turkey

3   Vocational School of Health Services, Department of Medical Imaging Techniques, Altinbas University, Istanbul, Turkey

4   Faculty of Engineering and Architecture, Department of Mechatronics Engineering, Nisantasi University, Istanbul, Turkey

Introduction

Adjuvant therapy with radioiodine is a standard procedure for differentiated thyroid cancer (DTC) and iodine-avid metastases. Most commonly, the administered ^{131}I activity is determined based on institutional guidelines of adequate dosage rather than individualized dose planning (Lassmann et al. 2010; Franzius et al. 2007). Benua et al. (1962) indicated that the blood dose should be used as surrogate for the bone marrow dose, and 2 Gy was identified as the threshold for severe hematologic toxicity. Treatment activity is usually determined by several strategies. Empiric dosage is the most common strategy for making decisions about the therapeutic activity in the advanced DTC. A broad range of fixed activities are commonly applied that

include the risk of exceeding bone marrow's dose limit (2 Gy) (Mazzaferri and Kloos 2001; Breitz et al. 1995). More recently, there is an increasing emphasis on personalized therapy for a safe and more effective therapy. Currently, there is no standardized way for estimating red bone marrow dose (Brans et al. 2007; Luster et al. 2008). The variety of dosimetry methods applied demonstrates the need for more clinical and dosimetric data with regard to red bone marrow dose estimation and toxicity levels. An important task in dosimetry is to periodically quantify the retained activity in the body of a patient by means of image analysis obtained from planar or hybrid imaging modalities. More recently, three-dimensional tomographic techniques become more and more available including pixel-wise attenuation correction and accurate quantification. Unfortunately, the dispersed nature of red bone marrow in the entire body complicates the direct quantification of red bone marrow uptake. Therefore, blood dose is increasingly used as a surrogate for red bone marrow dose (Chiesa et al. 2009). Accordingly, blood sampling and a series of whole-body scans made at multiple time points are required to accomplish blood dosimetry. However, the costs and required time involved consumption due to subsequent acquisitions hamper personalized dose planning. The dosimetry approaches discussed in the present study allow dose estimation to red bone marrow from the administration of therapeutic activities. Certainly, protocols of patient-specific dosimetry might allow an actual optimization of the therapy, but further efforts are required to improve the standards of dosimetry and its efficacy on the overall tumour response. The OLINDA/EXM 1.0 code has been increasingly utilized with user-friendly features to provide dose calculations for plenty of organs and hundreds of radionuclides (Stabin et al. 2005). More recently, OLINDA/EXM has been updated with a new version using the RADAR anthropomorphic phantom instead of the MIRD phantom that was used in the previous version. Likewise, several models have been introduced to calculate red bone marrow dose with different compensation for the red bone marrow self-dose and dose from source organs and remainder body (crossfire dose) (Hänscheid et al. 2013). Finally, IDAC-Dose 2.1 has been recently released to calculate absorbed dose based on earlier published SAF values for the ICRP adult computational voxel phantoms described in ICRP Publication 110 (ICRP 2009). This code also includes a representation for the circulating blood to perform dose estimation for 83 source organs and tissues irradiating 47 target organs and tissues with more than 1000 radionuclides published in ICRP Publication 107 (ICRP 2008).

The main goal of the current study was to find out the correlation between numerous dosimetry models including the readily available IDAC-Dose 2.1 and OLINDA/EXM codes. The study should also, if possible, identify the most reliable model for dosimetry-based therapy and explore the possibility to perform red bone marrow dosimetry excluding red bone marrow self-dose when blood sampling is impossible.

Materials and methods

Data collection

The present study included 18 patients (12 females and 6 males) suffering from metastatic differentiated thyroid cancer. All patients underwent the previous sessions of radioiodine therapy based on an empiric dose protocol. The age of the patients was 48 ± 16 years and the average Tg level was 398 ng/ml at the time of dosimetry. Blood test was requested to verify a TSH level above 30 µIU/ml before ^{131}I tracer administration.

The average mass and height of the patients were 78 ± 17 kg and 1.7 ± 0.1 m, respectively. The orally administered radiotracer of ^{131}I was 73 ± 16 MBq pursued by blood sampling (2 ml) and whole-body scans (WBSs) at several time points (2, 6, 24, 48, 72, and ≥ 96 h) as seen in Fig. 1.

When the scanning room was activity-free, a 1-min static image was acquired prior each scintigraphy for background correction. Anterior and posterior whole-body scans were obtained at 10 cm/min scan speed using a dual-head gamma camera equipped with a high-energy parallel hole collimator (Siemens Symbia T16, Erlangen, Germany). Camera settings were adjusted for scanning as followings: 364 keV energy photopeak, 15% window width, and matrix size of 256×1024. The body contour was delineated and the ROI's (regions of interest) counts were counted. The first whole-body scan at (2 h) was considered equal to 100% of the administered activity. The magnitude of remaining activity was estimated from the geometric mean of the corresponding counts to the initial count-activity proportion. Residence time (τ) was calculated by the following equation:

$$\tau = \tilde{A}/A_o \tag{1}$$

$$\tilde{A} = \int_{t=0}^{\infty} \left(A_o(t)\right) dt, \tag{2}$$

where τ is the residence time, $\tilde{A}$ the cumulative activity, and A_o the administered activity.

Blood specimens were measured using a well counter (Capintec. CRC25) which was calibrated for ^{131}I. An aliquot of 0.5 ml was withdrawn from each blood sample and then measured immediately. The sample was counted three times to reduce the counting errors, and the geometric mean of raw counts was corrected due to physical decay. The method reported by Pearson et al. (1995) was used to find the total blood volume (TBV$_{ml}$) as follows (Eqs. 3–5):

$$TBV_{ml}(\text{Male}) = ((1486 \times S) - 825) + (1578 \times S) \tag{3}$$

$$TBV_{ml}(\text{Female}) = ((1.06 \times \text{age}) + (822 \times S)) + [1395 \times S] \tag{4}$$

$$S = (W \times 0.425) \times (H \times 0.725) \times (0.007184), \tag{5}$$

where S is the surface area (cm^2), H the patient height (cm), and W the patient mass (kg).

Fig. 1 Solid line: bi-exponential fit of the mean ^{131}I activity retention (*y*-axis) as a function of time (*x*-axis) as derived from whole-body scans (WBSs) at different time points (2, 24, 48, 72, and 100 h). Dashed lines: bi-exponential fits of the standard deviation (± SD) of the ^{131}I activity retention as derived from the patient's data. Average SD was 9% (range 8–13%) for all time points
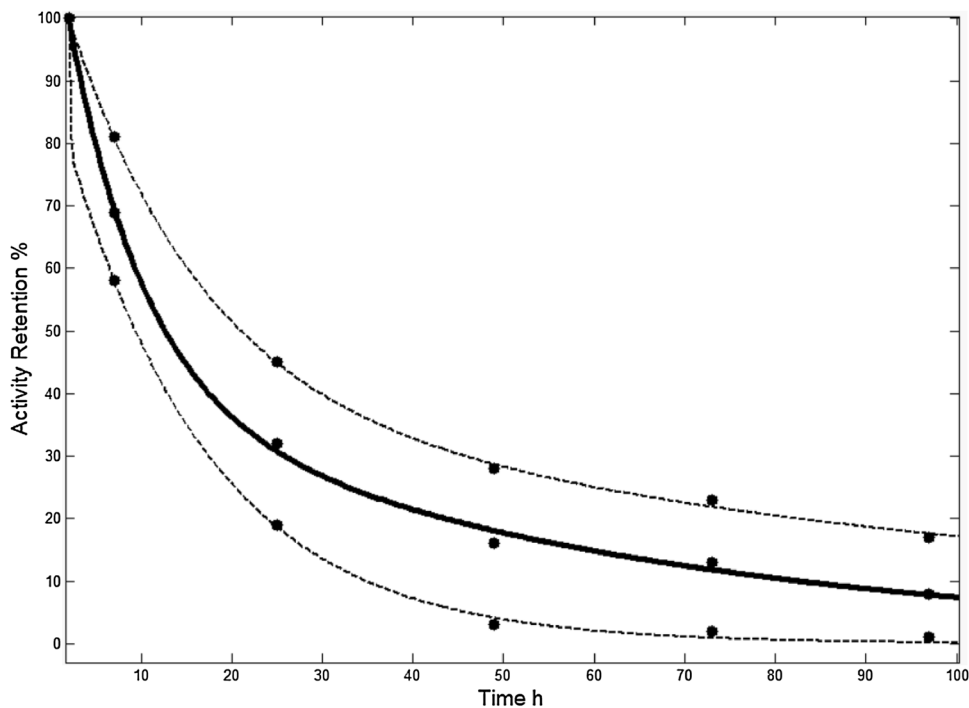
Red bone marrow-absorbed dose calculation

Various models were used to calculate doses of red bone marrow after ^{131}I administration.

OLINDA/EXM 1.0

Dose calculation was made by choosing the corresponding anthropomorphic phantom of the right gender. Then, the appropriate radioisotope was selected and the residence time was generated by a built in option (fit data to model) that allowed exponential fitting. A mass scale factor was used to calculated the mass of red bone marrow of the patient from that of the phantom, based on the ratio of patient mass/ phantom mass including red bone marrow.

IDAC-Dose 2.1

This computer program is based on the ICRP phantom from ICRP Publication 110 (ICRP 2009). IDAC incorporates a representation for the blood dose contribution to red bone marrow and enables calculating red bone marrow dose according to SAF tables reported in ICRP Publication 133 (ICRP 2016). Both dose components of crossfire and red bone marrow self-dose can be quantified by entering the residence time of ^{131}I in total blood and whole body. The red bone marrow mass of the patients was inserted according to the ratio between the mass of the patient and that of the adult reference phantom used in the program. The total red bone marrow dose was given in the results with two forms. The first one was using total body and blood parameters in the program (TD) and the second way (TDrm) was achieved by deriving red bone marrow residence time from the blood circulation (via IDACBLood model built in the code) besides to the total body dose contribution.

Model by Traino et al. (Traino Model)

Traino et al. (2007) provided different model with a nonlinear mass scaling factor for red bone marrow self-dose and crossfire dose:

$$D_{\text{Rm}} = [\tilde{A}\text{bl}] \times m_{\text{Rm}} \times \text{RMBLR} \times S_{\text{Rm} \leftarrow \text{Rm}} \times \left(\frac{\text{mTB}}{\text{mtb}} \right)^{x3} + \left(\tilde{A}_{\text{tb}} - [\tilde{A}\text{bl}] \times m_{\text{Rm}} \times \frac{\text{mtb}}{\text{mTB}} \times \text{RMBLR} \right)$$
$$\times \left\{ S_{\text{Rm} \leftarrow \text{TB}} \times \left(\frac{\text{mTB}^2}{\text{mtb} \times \text{mRB}} \right)^{x1} \left(\frac{\text{mTB}}{\text{mtb}} \right)^{x2} - S_{\text{Rm} \leftarrow \text{Rm}} \times \left(\frac{\text{mTBmRm}^2}{\text{mtbmRB}^2} \right)^{x3} \right\}$$

(6)

where D_{Rm} is the red bone marrow dose, $[\tilde{A}bl]$ the concentration of cumulative activity in blood, m_{Rm} the red bone marrow mass of standard male and female phantoms (1.12 kg for males, and 1.3 kg for females), RMBLR the red bone marrow-to-blood ratio [0.19/(1 − HCT); HCT: patient-dependent haematocrit value], $S_{Rm \leftarrow Rm}$ the bone marrow to bone marrow S factor (for males: 1.55×10^{-5} mGy/MBq.s; for females: 1.41×10^{-5} mGy/MBq.s), $\tilde{A}_{tb}$ the total body cumulative activity, m_{tb} the patient mass, m_{TB} the standard phantom mass (for male: 73.7 kg; for female 56.9 kg), $S_{Rm \leftarrow TB}$ the total body to bone marrow S factor (for males: 6.29×10^{-7} mGy/MBq.s, for female: 7.72×10^{-7} mGy/MBq.s), and m_{RB} the standard phantom's remainder of body mass ($m_{RB} = m_{TB} - m_{Rm}$), and values of x_1, x_2, and x_3 are 0.50, 0.831, and 0.974 for males, and 0.47, 08.02, and 0.972 for females.

Model by Siegel et al. (Siegel Model)

Siegel (2005) offered a two-component model including a blood-based method for red bone marrow self-dose estimation (Eq. 7):

$$D_{RM} = 0.00000515 \times \left\{ [\tilde{A}_{bl}] + [\tilde{A}_{wb}] \times 7.5 \right\}, \tag{7}$$

where D_{RM} is the red bone marrow dose (mGy), $[\tilde{A}_{bl}]$ the blood cumulative activity concentration (MBq s/Kg), and $[\tilde{A}_{wb}]$ the total body cumulative activity concentration (MBq s/Kg).

Revised Sgouros Model (RSM)

Wessels et al. (2004) provided a mathematical model for dose calculation in radio-labelled antibody therapy relying on the MIRD (Medical Internal Radiation Dosimetry) scheme. A standardized approach was added to account for the variations in patient mass for the body remainder dose component. To simplify the clinical implementation, regional marrow uptake and time-dependent changes in the marrow–blood concentration ratio were not included. Equation 8 illustrates the process of red bone marrow dose calculation:

where $\tilde{A}_{bl}$ is the cumulative activity in the blood, HCT the haematocrit value, $S_{(RM \leftarrow RM)}$ the red bone marrow self-dose factor for male phantom (1.725×10^{-5} mGy/MBq.s), M_{wb} the patient mass, $\tilde{A}_{wb}$ the total body cumulative activity, $[\tilde{A}_{bl}]$ the blood cumulative activity concentration [kg^{-1}], and $S_{(Rm \leftarrow WB)}$ the S value of whole body to red bone marrow dose. Willegaignon et al. (2012) reported a correction on the S value of the remainder body when using the Sgouros model; $S_{(Rm \leftarrow RB)}$ was expressed as ($3.26 \times 10^{-5}/M_{wb\ patient}$).

Model by Sui Shen et al. (Shen Model)

Shen et al. (1999) provided a model (Eq. 9) where RMBLR can be derived from patient's haematocrit and RM extracellular fluid fraction:

$$D_{RM}(rad/mCi) = 0.313 \times RMBLR \times C_{blood} + 0.456 \times \tilde{A}_{TB}/m_{TB}, \tag{9}$$

where C_{blood} is the cumulated radioactivity concentration (µCi-h/mL) in blood, $\tilde{A}_{TB}$ the cumulated activity (µCi-h) in total body, m_{TB} the patient's real body mass (g), RMBLR the red bone marrow-to-blood ratio [RMBLR = 0.19/(1 − HCT); HCT: patient-dependent haematocrit value].

Model by De Keizer et al. (Keizer Model)

De Keizer et al. (2004) suggested the following model (Eq. 10):

$$
\begin{aligned}
D_{RM} &= D_{RM}^{\ blood} + D_{Rm}^{\ TB} \\
&= A_0[\tau]\, m^{RM}_{(model)} \frac{mTBPatient}{mTB\ model} \frac{RMECFF}{1 - HCT} \times S_{(RM \leftarrow RM)} \\
&+ A_0 \tau_{TB} \frac{mTB\ (model)}{mTB\ (patient)} \times S_{Rm \leftarrow TB}, \tag{10}
\end{aligned}
$$

where D_{RM} is the red bone marrow dose, $D_{RM}^{\ blood}$: the blood self-dose, $D_{Rm}^{\ TB}$ the red bone marrow dose from the entire body, $[\tau]$ the residence time (h: hour) of the blood concentration (L), $m^{RM}_{(model)}$ the red bone marrow mass of body phantom (1.120 kg), and mTB the patient and phantom total

$$
\begin{aligned}
D_{Rm} &= D_{Rm}(self) + D_{Rm}(cross) \\
D_{Rm}(self) &= \tilde{A}_{bl} \times \frac{RMECFF}{1 - HCT} \times \left(\frac{1.5}{5.2}\right) \times S_{RM \leftarrow RM} \times \frac{70}{Mwb\ patient} \\
D_{Rm\ cross} &= \left\{ \tilde{A}_{wb} - [\tilde{A}_{bl}] \times \frac{RMECFF}{1 - HCT}\left(\frac{1.5}{70}\right) \times M_{wb} \right\} \times S_{(Rm \leftarrow RB)} \\
S_{(Rm \leftarrow RB)} &= S_{RM \leftarrow WB} \times \left(\frac{1}{1 - \left(\frac{1.5}{70}\right)}\right) - S_{RM \leftarrow RM} \times \left(\frac{\left(\frac{1.5}{70}\right)}{1 - \left(\frac{1.5}{70}\right)}\right),
\end{aligned}
\tag{8}
$$

body mass (MIRD phantom: 73.7 kg), RMECFF the red bone marrow extracellular fluid fraction, and HCT the volume fraction of red blood cells.

In Eq. 10, $S_{Rm \leftarrow Rm}$ is the red bone marrow self-dose S value for ^{131}I (1.55×10^{-5} mGy/MBq.s) and $S_{Rm \leftarrow TB}$ is the total body to red bone marrow S value (2.78×10^{-7} mGy/MBq s).

EANM-modified Model

Lassmann et al. (2008) published the EANM (European Association of Nuclear Medicine) guidelines for dosimetry including the model given in Eq. 11 to be conservatively used in dose calculation (Gy/GBq):

$$D_{rm}/A_0 = 61 \times \tau_{\text{blood ml (h)}} + \left(\frac{0.106}{wt}\right) \times \tau_{\text{total body (h)}}, \quad (11)$$

where D_{rm}/A_0 is the absorbed dose to red bone marrow per administered activity, τ_{ml} (h) the residence time in 1 ml blood, $\tau_{\text{total body (h)}}$ the total body residence time, and wt the body mass.

Single Measurement (SMM) Model

If Eq. 12 holds:

$$\tau_{\text{blood ml (h)}} = \frac{0.17}{TBV} \times \tau_{\text{total body (h)}} \quad \text{and} \quad \tau_{\text{total body (h)}} = \frac{48}{\ln(AT)}, \quad (12)$$

where (AT) is the activity retention (%) (Hänscheid et al. 2009).

Then, Eqs. 11 and 12 can be joined to estimate blood dose from one measurement (3):

$$D_{rm}/A_0 = \left[61 \times \frac{0.17}{TBV} \times \tau_{\text{total body (h)}}\right] + \left[\left(\frac{0.106}{wt}\right) \times \frac{48}{\ln(AT)}\right], \quad (13)$$

where D_{rm}/A_0 is the absorbed dose per administered activity (Gy/GBq), τ_{ml} (h) the residence time in 1 ml blood, $\tau_{\text{total body (h)}}$ the total body residence time, wt the body mass, (0.17) is the average ratio of the blood residence time to the total body residence time of the participant patients, and TBV is the total blood volume.

Statistical analysis

All results are reported by mean, minimum, maximum, and standard deviation values. Shapiro–Wilk test was used for exploring whether the data follow a normal distribution. Accordingly, the non-parametric Mann–Whitney U test was applied to determine any significant difference between the groups using the SPSS 15.0 software (SPSS Complex Samples™ 15.0 Copyright © 2006 by SPSS Inc., USA) with 95% confidence levels.

Table 1 Red bone marrow-absorbed dose (mGy) calculated from several dosimetry models

Patient	A_0	Traino	RSM	Siegel	Shen	Keizer	OLINDA	EANM	SMM
1	103.6	7.4	9.1	9.7	9.7	6.0	10.2	10.4	13
2	61.4	2.5	3.0	1.9	3.2	2.3	2.2	4.8	1.0
3	74	3.2	3.9	3.1	3.9	2.6	3.6	5.0	5.0
4	18.5	1.8	2.2	1.1	2.3	1.4	1.3	1.7	4.7
5	66.6	1.8	2.2	1.7	2.4	1.6	1.9	3.3	5.0
6	76.2	2.1	2.6	2.5	2.8	1.9	2.4	3.6	5.6
7	78.8	3.7	4.4	3.7	4.8	3.3	3.5	6.2	6.6
8	87.0	2.7	3.1	2.2	3.4	3.0	3.7	3.9	3.5
9	79.6	3.6	4.2	2.4	4.6	3.1	2.3	7.2	6.2
10	71.8	4.3	5.2	4.2	5.3	3.6	4.8	6.9	6.2
11	74.0	7.6	9.3	8.9	10.0	6.2	9.5	11.2	11.1
12	72.2	4.3	5.1	4.2	5.7	3.7	4.5	8.0	10.2
13	82.9	7.0	8.0	7.3	9.2	6.7	7.5	12.1	9.0
14	66.6	4.1	5.1	3.5	5.0	3.4	4.1	7.9	7.4
15	78.4	5.4	6.8	4.3	7.0	3.9	5.2	10.5	8.7
16	87.7	4.8	5.8	4.1	6.2	4.2	4.4	10.1	8.9
17	69.6	3.8	5.1	2.5	4.8	3.0	3.2	8.0	7.6
18	70.3	3.1	3.8	2.8	3.7	2.3	3.1	5.0	6.0
Mean	73.3	4.1	4.9	3.9	5.2	3.5	4.3	7.0	6.8
SD	16.3	1.7	2.1	2.3	2.3	1.5	2.4	2.9	2.5

A_0 administered activity (MBq), *RSM* Revised Sgouros Model

Table 2 Red bone marrow dose (mGy/MBq) generated by IDAC-Dose 2.1

Patient	Crossfire dose	TD	TD_{rm}
1	16.0	17.1	10.2
2	3.3	4.6	2.6
3	5.0	6.1	3.6
4	1.5	1.9	1.1
5	2.9	3.8	2.1
6	3.9	4.9	2.8
7	7.2	8.9	5.3
8	5.9	7.0	4.2
9	3.8	5.6	2.8
10	7.6	9.2	5.4
11	14.7	16.6	9.7
12	7.0	9.5	5.1
13	16.5	19.8	9.3
14	5.7	7.9	4.4
15	4.9	7.9	3.9
16	7.2	10.9	5.5
17	3.4	5.5	3.0
18	3.9	5.3	2.9
Mean	6.5	8.5	4.6
SD	4.4	4.7	2.6

TD total dose including self-dose from blood and crossfire dose from total body per administered activity (A_0), *TD_{rm}* total dose including self and crossfire dose per administered activity (A_0) from red bone marrow activity (derived from the circulating blood activity) and the remaining body

Results

Tables 1, 2 show the red bone marrow doses from all the dosimetry models as described in the methodology. Table 2 summarizes the total red bone marrow dose generated by the IDAC-Dose 2.1 program with two types of data input including red bone marrow self-dose surrogated by blood and the other with deriving the red bone marrow activity portion from the circulating blood, plus the cross fire dose component for both types. Among the results generated by IDAC-Dose 2.0 code, it was demonstrated that the accumulated activity fraction of the red bone marrow was 0.2 ± 0.10 from the circulating blood and the proportion of the corresponding residence time was 0.04 ± 0.005 from that of the total blood. Upon to Table 1, EANM model was highly varied from the reference model with respect to the absolute values of red bone marrow dose. In addition, attempt was made to provide analytical comparison between these models. The degree of deviation in red bone marrow dose between most of the models as compared to the Revised Sgouros model is summarized in Table 3 and illustrated in Fig. 2. The minimum deviation among these models was observed in the Traino, OLINDA/EXM 1.0, IDAC-Dose

Table 3 Deviation of the results (%) obtained with various dosimetry models to those obtained with the reference model (Revised Sgouros Model)

Dosimetry model	Mean	SD	Min/Max[b]	P_{value}[a]
Traino et al.	−17	3	−25/−12	0.18
Siegel et al.	−24	16	−50/7	0.06
Shen et al.	6	5	−5/16	0.74
Keizer et al.	−29	9	−42/−1.3	0.03
OLINDA/EXM	−15	17	−37/21	0.26
IDAC-DOSE 2.1[c]	−8[c]	23[c]	−52/36[c]	0.6[c]/0.4[d]
SMM	48	45	−67/127	0.02
EANM	40	23	−23/74	0.04

[a]*CI* confidence interval 95%. Mann–Whitney *U* (*t*) test

[b]Min/Max: minimum deviation/maximum deviation

[c]Results refer to TDrm (Table 2)

[d]*P* value for the crossfire dose section in Table 2

2.0, and Shen models. Table 3 also incorporates the mean, minimum, and maximum deviation percentages for each dosimetry model as compared to the reference RSM model. The calculated absorbed dose using the EANM code and the single measurement based (48 h) SMM model shows moderate correlation ($R^2 = 0.63$), as shown in Fig. 3, and there was no statistical difference in red bone marrow dose between IDAC 2.1 (TD section) and EANM. Similarly, the correlation between OLINDA/EXM 1.0 and EANM was not strong ($R^2 = 0.52$) as shown in Fig. 4. In contrast, Fig. 5 exhibits pretty strong association between the results of the Traino and Revised Sgouros models ($R^2 = 0.99$), similar to the correlation between the results of the OLINDA/EXM and Revised Sgouros models, and those the Traino and OLINA/EXM 1.0 models ($R^2 = 0.90$ and 0.91, respectively; Fig. 6). Interestingly, the Shen model which is considered a simple estimation model shows a robust correlation with more complex models like the Revised Sgouros model ($R^2 = 0.98$), as shown in Fig. 7. The results obtained with the IDAC-Dose 2.1 and OLINDA/EXM 1.0 models agreed very well, in terms of the red bone marrow cross fire dose ($R^2 = 0.90$) as illustrated in Fig. 8, and also the results of the total red bone marrow dose (TD_{rm}) were highly correlated to the reference RSM model, as shown in Fig. 9.
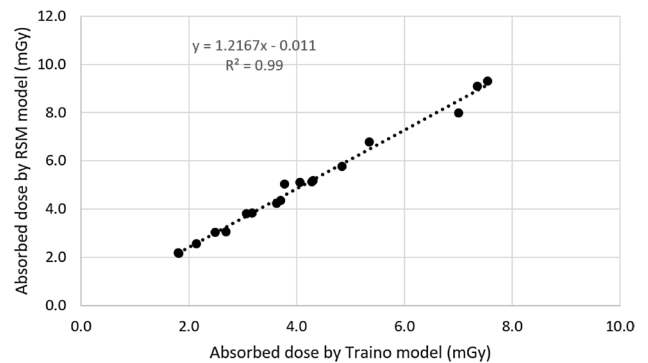
Discussion

Radioiodine (^{131}I) is the most common radionuclide applied for metastatic DTC therapy all over the world. Particularly, distant metastatic thyroid cancer requires a large activity administration to achieve satisfactory treatment, but, at the same time, toxicity risk should be kept as low as possible (Salvatori and Luster 2010; Lassmann et al. 2010). At
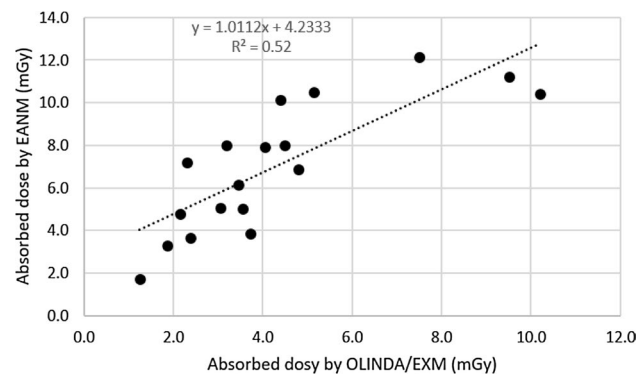
Fig. 2 Deviation of red bone marrow dose estimated by means of several dosimetry models as compared to the RSM model
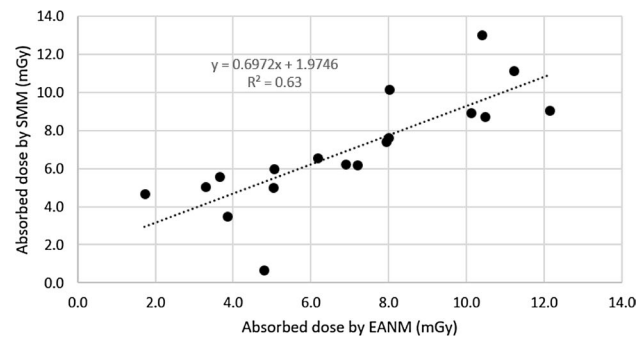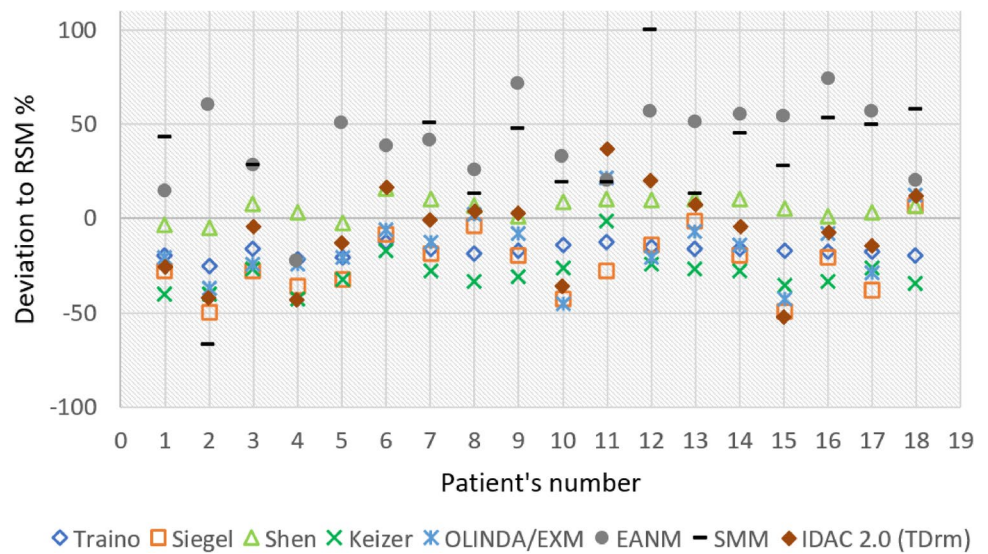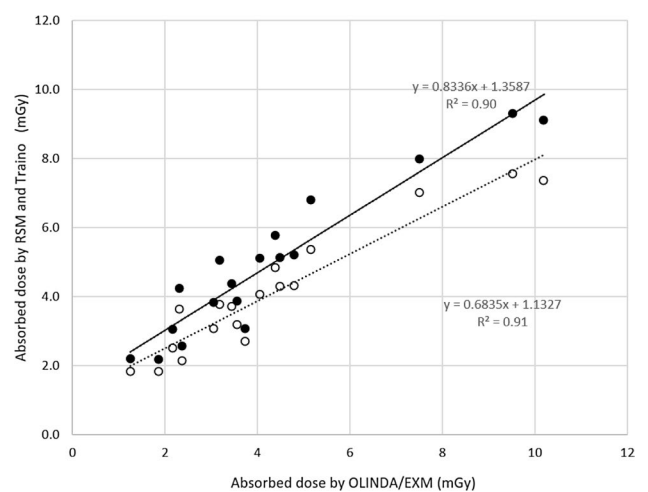

Fig. 3 Correlation between red bone marrow-absorbed dose (mGy) calculated with the EANM and SMM models, for the investigated 18 patients
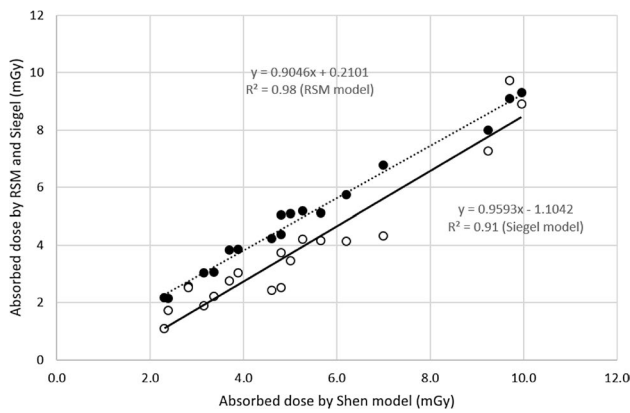
Fig. 4 Correlation between red bone marrow-absorbed dose (mGy) calculated with the EANM and OLINDA/EXM 1.0 models, for the investigated 18 patients

Fig. 5 Correlation between red bone marrow-absorbed dose (mGy) calculated with the RSM and Traino models, for the investigated 18 patients
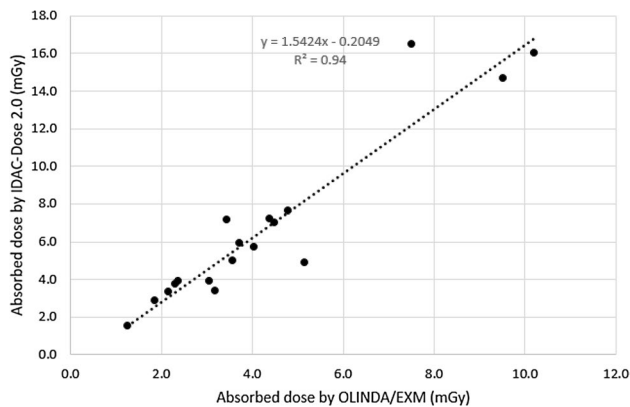
Fig. 6 Correlation between red bone marrow-absorbed dose (mGy) calculated with the Traino (open circles, dashed line) and RSM models (full circles, solid line) as compared with that calculated with OLINDA/EXM 1.0, for the investigated 18 patients

present, determination of a maximum safe activity is considered as the best choice for optimizing treatment and minimizing adverse effects to blood-forming stem cells. Over the last 2 decades, many models have been developed for red

Fig. 7 Correlation between red bone marrow-absorbed dose (mGy) calculated with the Shen (full circles, dashed line) and Siegel (open circles, solid line) models with those calculated with the RSM model, for the investigated 18 patients

Fig. 8 Correlation between red bone marrow crossfire dose (mGy) calculated by the OLINDA/EXM 1.0 and IDAC-DOSE 0.2 models, for the investigated 18 patients
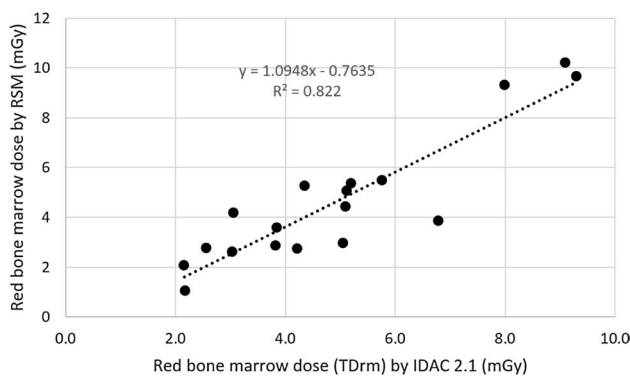
Fig. 9 Correlation between red bone marrow dose (mGy) calculated by RSM and IDAC-DOSE 0.2 models (TD_{rm}), for the investigated 18 patients

bone marrow dose estimates. One of the most challenging problems in red bone marrow dose calculation is the fact that red bone marrow is distributed in multiple regions within the body rather than in one organ (Bernier et al. 2001; Siegel et al. 1999). This makes the activity quantitation quite difficult and led to the concept that red bone marrow self-dose can be estimated through the blood dose which should be less than or equal to 2 Gy. The current guidelines of the European Association of Nuclear Medicine (EANM) suggest the use of the total cumulative activity in the blood for an estimate of self-marrow dose (Hindorf et al. 2010). In contrast, the models implemented in the present study consider partial blood activity contribution to red bone marrow dose. EANM justified using the total blood activity by the fact that the size of the iodine molecule is larger than that of monoclonal antibodies.

One of the purposes of the present study was to compare the performance of available dosimetry models via realistic dosimetry data. The OLINDA/EXM 1.0 code is utilized worldwide for internal dose assessment in radiopharmaceutical procedures using the classic MIRD phantom. This phantom is known as the so-called stylized phantom with mathematically defined organs and tissues occupying finite spaces in the body. The new version of OLINDA/EXM (version 2.0) implements more realistic anatomic models (NURBS phantoms) based on non-uniform rational b-spline modelling techniques, to define reference male and female phantoms using the defined organ masses given in ICRP publication 89 (ICRP 2002). In the IDAC-Dose 2.1 program, the MIRD phantom was also replaced by a more realistic phantom, i.e., by the computational voxel phantoms described in ICRP Publication 110, also including further biokinetic models to describe the uptake, distribution, and retention of radiopharmaceuticals within the human body. Furthermore, most of the models involve calculating red bone marrow's self-dose plus crossfire dose from the remaining body dose. In the present study, the Revised Sgouros Model (RSM) was selected as a reference model, because it has been tested in multicentre comparison studies (Wessels et al. 2004). This model also includes the standard MIRD approach for the dose contribution from the remainder body to red bone marrow dose, and an additional correction was included to account for variations in patient mass (Wessels et al. 2004). In the present study, for the first time, an attempt was made to evaluate the correlation between the red bone marrow crossfire dose as calculated with OLINDA\EXM, and the dose to the blood calculated by various models. As a result, the statistical analyses performed in the present study did not demonstrate any statistically significant difference between the results of the Revised Sgouros Model and those of the OLINDA/EXM, Shen, Traino, IDAC-Dose 2.1 (TD_{rm} and crossfire dose), and Siegel models (t test; $p_{value} > 0.05$). In contrast, a significant difference was observed between the results of the

RSM and those of the Keizer's, EANM, IDAC-Dose 2.1(TD section), and SMM models (*t* test; $p_{value} < 0.05$). The recent model of Traino involves a nonlinear $S_{TARGET \leftarrow SOURCE}$ scaling factor instead of the linear approximation usually used, to obtain a more accurate estimation for the self-irradiation and cross-irradiation dose components. However, the dose values obtained in the present study with the Traino model showed a strong association with those calculated with the RSM and OLINDA/EXM models ($R^2 = 0.98$ and 0.92, respectively). In contrast, the simple analytical model by Shen et al. (1999) showed a surprisingly good agreement with more advanced models like the RSM ($R^2 = 0.98$, $p_{value} > 0.05$) and Traino model ($p_{value} > 0.05$). All the models investigated here involved red bone marrow self-dose plus gamma dose contributions except for the OLINDA/EXM code. The agreement between the dose values generated by OLINDA/EXM and those obtained with the other blood-based models suggests that the crossfire dose can be used for activity dose planning when blood sampling is impossible. Similarly, the results of the IDAC-Dose 2.1 code showed a robust association with those from the OLINDA/EXM 1.0 code in terms of red bone marrow crossfire dose ($R^2 = 0.94$ and $p_{value} > 0.05$). The small variation observed is attributed to the different reference phantoms and dose fractions used in the codes. Table 2 illustrates higher dose values for the ICRP phantom compared to those for the other models owing to the underestimation of the *S* values when using the Snyder phantom. A substantial variation in the dose fractions was also reported for various source and target organs between ICRP voxel class phantoms and the stylised model, due to differences in organ morphology and different distances between source and target tissues within the body.

In the present study, red bone marrow dose from a single measurement was also compared to that obtained with the EANM model, but the resulting correlation was only modest ($R^2 = 0.63$). However, it might be worth of developing alternative simplified models that make dose assessment easier and more convenient.

In the same context, the Council of the European Union issued a new directive regarding all the types of radiation therapy. The directive states (Article 56—Paragraph 1) that exposure and dose optimization in all radio-therapeutic procedures shall be planned individually with respect to the ALARA principle (ALARA: As Low As Reasonably Achievable) by 2018 (Council of the European Union 2013). Accordingly, this directive supports applying dosimetry in targeted radionuclide therapy. Particularly, metastatic thyroid cancer therapy implies the administration of large activities for successive treatment. Because metastatic lesions are difficult to detect and measure by radiotracers, the accuracy of dose prediction for these lesions is limited. As an alternative, activity could be administered therapeutically according to the maximum safe activity for the most critical tissues

or organs. Owing to that, the therapeutic activity used in radioiodine treatment can be administered up to the red bone marrow dose limit. Some studies highlighted the outcome of dosimetry-oriented therapy as compared to the fixed activity approach (Lee et al. 2008; Klubo et al. 2011). More recently, it was advocated that dosimetry-based ^{131}I therapy seems more effective in improving treatment outcome and overall survival in advanced differentiated thyroid cancer, with an emphasis on the need for more controled studies regarding the efficacy and the benefits of radioiodine therapy when relying on the tolerated dose of bone marrow.

In summary, it is a fact dosimetry still requires a long time and large effort for blood sampling and imaging, i.e., up to a couple of days. However, the strong correlation between the results from OLINDA/EXM and IDAC-Dose 2.1 with those from other blood-based models will support reasonable and costless dose planning. As a result, routine dosimetry implementation in radioiodine therapy of metastatic DTC will be easier with readily available methods.

Conclusion

Results from most of the dosimetry models investigated in the present study did not show any significant difference with those from the Revised Sgouros Model, and they showed good agreement with doses obtained with the OLINDA/EXM and IDAC-Dose 2.1 software. The present study emphasizes the feasibility of the IDAC-Dose 2.1 code for dose calculations using ICRP reference voxel phantoms.

Compliance with ethical standards

Conflict of interest All authors declare that there is no conflict of interest that could be perceived as prejudicing the impartiality of the research reported.

Ethical approval All procedures performed in the current study involving human participants were in accordance with the ethical standards of the institutional and/or national research committee and with the 1964 Helsinki declaration and its later amendments or comparable ethical standards. Istanbul University Cerrahpaşa Medical Faculty Clinical Research Ethics Committee approved this study (document number: 83045809/604/02-8877).

Informed consent Informed consent was obtained from all the individual participants included in the study.

References

Andersson M, Johansson L, Eckerman K, Mattsson S (2017) IDAC-Dose 2.1, an Internal dosimetry program for diagnostic nuclear medicine based on the ICRP adult reference voxel phantoms. EJNMMI Res 7(1):88

Benua RS, Cicale NR, Sonenberg M, Rawson RW (1962) The relation of radioiodine dosimetry to results and complications in the treatment of metastatic thyroid cancer. Am J Roentgenol Radium Ther Nucl Med 87:171–182

Bernier O, Leenhardt L, Hoang C, Aurengo A, Mary JY, Menegaux F, Enkaoua E, Turpin G, Chiras J, Saillant G, Hejblum G (2001) Survival and therapeutic modalities in patients with bone metastases of differentiated thyroid carcinomas. J Clin Endocrinol Metab 86:1568–1573

Brans B, Bodei L, Giammarile F, Linden O, Luster M, Oyen G, Tennvall J (2007) Clinical radionuclide therapy dosimetry: the quest for the "Holy Gray". Eur J Nucl Med Mol Imaging 34:772–786

Breitz B, Durham JS, Fisher DR, Weiden PL, DeNardo GL, Goodgold HM, Nelp WB (1995) Pharmacokinetics and normal organ dosimetry following intraperitoneal rhenium-186-labeled monoclonal antibody. J Nucl Med 36:754–761

Chiesa C, Castellani MR, Vellani C, Orunesu E, Negri A, Azzeroni R, Botta F, Maccauro M, Aliberti G, Seregni E, Lassmann M, Bombardieri E (2009) Individualized dosimetry in the management of metastatic differentiated thyroid cancer. Q J Nucl Med Mol Imaging 53:546–561

Council of the European Union (2013) Council Directive 2013/59/EURATOM. Off J Eur Union 56:216

De Keizer B, Hoekstra A, Konijnenberg MW, Devos F, Lambert B, Van RP, Lips M, de Klerk JH (2004) Bone marrow dosimetry and safety of high 131I activities given after recombinant human thyroid-stimulating hormone to treat metastatic differentiated thyroid cancer. J Nucl Med 45:1549–1554

Franzius C, Dietlein M, Biermann MF, Fruhwald M, Linden T, Bucsky P, Reiners C, Schober O (2007) Procedure guideline for radioiodine therapy and 131iodine whole-body scintigraphy in paediatric patients with differentiated thyroid cancer. Nuklearmedizin 46(5):224–231

Hänscheid H, Lassmann M, Luster M, Kloos RT, Reiners C (2009) Blood dosimetry from a single measurement of the whole body radioiodine retention in patients with differentiated thyroid carcinoma. Endocr Relat Cancer 16:1283–1289

Hänscheid H, Canzi C, Eschner W, Flux G, Luster M, Strigari L, Lassmann M (2013) EANM dosimetry committee series on standard operational procedures for pretherapeutic dosimetry II. Dosimetry prior to radioiodine therapy of benign thyroid diseases. Eur J Nucl Med Mol Imaging 40:1126–1134

Hindorf C, Glatting G, Chiesa C, Lindén O, Flux G (2010) EANM dosimetry committee guidelines for bone marrow and whole-body dosimetry. Eur J Nucl Med Mol Imaging 37(4):821–828

ICRP (2002) Basic anatomical and physiological data for use in radiological protection reference values. ICRP Publication 89. Annals of ICRP, vol 32, issue 3–4

ICRP (2008) Nuclear Decay Data for Dosimetric Calculations. ICRP Publication 107. Annals of ICRP, vol 38, issue 3

ICRP (2009) Adult Reference Computational Phantoms. ICRP Publication 110. Annals of ICRP, vol 39, issue 2

ICRP (2016) The ICRP computational framework for internal dose assessment for reference adults: specific absorbed fractions. ICRP Publication 133 Ann ICRP 45(2):1–74

Klubo-Gwiezdzinska J, Van Nostrand D. Atkins F, Burman K, Jonklaas J, Mete M, Wartofsky L (2011) Efficacy of dosimetric versus empiric prescribed activity of 131I for therapy of differentiated thyroid cancer. J Clin Endocrinol Metab 96:3217–3225

Lamart S, Bouville A, Simon SL, Eckerman KF, Melo D, Lee C (2011) Comparison of internal dosimetry factors for three classes of adult computational phantoms with emphasis on I-131 in the thyroid. Phys Med Biol 56(22):7317–7335

Lamart S, Simon SL, Bouville A, Moroz BE, Lee C (2016) S values for 131I based on the ICRP adult voxel phantoms. Radiat Prot Dosim 168(1):92–110

Lassmann M, Hänscheid H, Chiesa C, Hindorf C, Flux G, Luster M (2008) EANM Dosimetry Committee series on standard operational procedures for pre-therapeutic dosimetry I: blood and bone marrow dosimetry in differentiated thyroid cancer therapy. Eur J Nucl Med Mol Imaging 35:1405–1412

Lassmann M, Reiners C, Luster M (2010) Dosimetry and thyroid cancer: the individual dosage of radioiodine. Endocr Relat Cancer 17(3):R161–R172

Lee JJ, Chung JK, Kim SE, Kang WJ, Park DJ, Lee DS, Cho BY, Lee MC (2008) Maximal safe dose of I-131 after failure of standard fixed dose therapy in patients with differentiated thyroid carcinoma. Ann Nucl Med 22:727–734

Luster M, Clarke SE, Dietlein M, Lassmann M, Lind P, Oyen WG, Tennvall J, Bombardieri E (2008) Guidelines for radioiodine therapy of differentiated thyroid cancer. Eur J Nucl Med Mol Imaging 35(10):1941–1959

Mazzaferri EL, Kloos RT (2001) Clinical review 128: Current approaches to primary therapy for papillary and follicular thyroid cancer. J Clin Endocrinol Metab 86(4):1447–1463

Pearson TC, Guthrie DL, Simpson J, Chinn S, Barosi G, Ferrant A, Lewis SM, Najean Y (1995) Interpretation of measured red cell mass and plasma volume in adults: Expert Panel on Radionuclides of the International Council for Standardization in Haematology. Br J Haematol 89:748–756

Salvatori M, Luster M (2010) Radioiodine therapy dosimetry in benign thyroid disease and differentiated thyroid carcinoma. Eur J Nucl Med Mol Imaging 37(4):821–828

Shen S, DeNardo GL, Sgouros G, O'Donnell RT, DeNardo SJ (1999) Practical determination of patient-specific marrow dose using radioactivity concentration in blood and body. J Nucl Med 40:2102–2106

Siegel JA (2005) Establishing a clinically meaningful predictive model of hematologic toxicity in nonmyeloablative targeted radiotherapy: practical aspects and limitations of red marrow dosimetry. Cancer Biother Radiopharm 20:126–140

Siegel JA, Thomas SR, Stubbs JB, Stabin MG, Hays MT, Koral KF, Robertson JS, Howell RW, Wessels BW, Fisher DR, Weber D, Brill B (1999) MIRD pamphlet no. 16: Techniques for quantitative radiopharmaceutical biodistribution data acquisition and analysis for use in human radiation dose estimates. J Nucl Med 40:37S– 61S

Stabin MG, Parks RB, Crowe E (2005) OLINDA/EXM: the second-generation personal computer software for internal dose assessment in nuclear medicine. J Nucl Med 46:1023–1027

Stabin MG, Xu X, Emmons M, Segars W, Shi C, Fernald J (2012) RADAR reference adult, pediatric, and pregnant female phantom series for internal and external dosimetry. J Nucl Med 53(11):1807–1813

Traino AC, Ferrari M, Cremonesi M, Stabin MG (2007) Influence of total-body mass on the scaling of S -factors for patient-specific, blood-based red-marrow dosimetry. Phys Med Biol 52:5231–5248

Verburg F, Markus L, Luca G, Michael L, Carlo C, Nicolas C, Glenn F (2017) The 'reset Button' revisited: why high activity 131i therapy of advanced differentiated thyroid cancer after dosimetry is advantageous for patients. Eur J Nucl Med Mol Imaging 44(6):915–917

Wessels BW, Bolch WE, Bouchet LG, Breitz HB, Denardo GL, Meredith RF, Stabin MG, Sgouros G (2004) Bone marrow dosimetry using blood-based models for radiolabeled antibody therapy: a multiinstitutional comparison. J Nucl Med 45:1725–1733

Willegaignon J, Sapienza MT, Buchpiguel CA (2012) Comparison of different dosimetric methods for red marrow absorbed dose calculation in thyroid cancer therapy. Radiat Prot Dosim 149:138–146